

DEMONSTRATION OF FLAT ION BEAM-CREATION AND -INJECTION INTO A SYNCHROTRON

L. Groening, S. Appel, L. Bozyk, Y. El-Hayek, M. Maier, C. Xiao, GSI, 64291 Darmstadt, Germany

Abstract

An ion beam with different horizontal and vertical emittances has been created from a beam with initially equal emittances. This round-to-flat adoption has been accomplished without any beam loss. In the set-up the beam passes through a stripping foil placed inside a solenoid followed by a skewed quadrupole triplet. The amount of beam flatness has been controlled by setting the solenoid field strength only. Increase of the product of the two transverse emittances is purely due to the stripping process that occurs anyway along an ion linac. Beams with different amounts of flatness were injected into a synchrotron applying horizontal multi-turn injection. The efficiency of injection increased as smaller as the horizontal emittance was set by the round-to-flat adaptor.

INTRODUCTION

For heavy-ion synchrotrons an efficient Multi-Turn Injection (MTI) from the injector linac is crucial in order to reach the specified currents using the available machine acceptance. The FAIR Heavy-ion synchrotrons are operated with intermediate charge state ions in order to increase the space charge limit. Therefore, stripping injection is not an option and the MTI has to respect Liouville's theorem for the chosen charge state - avoiding the already occupied phase space area. To achieve the space charge limit the multiplication of the injected current should be as large as possible. The beam loss during the MTI must not exceed the limits determined by machine protection and by the vacuum requirements. Especially for low energy and intermediate charge state ions, the beam loss can cause a degradation of the vacuum and a corresponding reduction of the beam lifetime.

One consequence of single-plane MTI is that the effective acceptance in the injection plane (usually the horizontal one) is reduced w.r.t. the acceptance in the other transverse plane. However, the two transverse emittances of the injected beam are generally similar to equal. The case may rise that the injected beam emittance is within the vertical acceptance budget but not within the horizontal acceptance budget for high MTI performance, although the product of its two emittances is lower than the product of the two effective acceptances. The MTI performance is thus reduced due to a not favourable emittance partitioning of the injected beam rather than by the product of its two emittances. Re-partitioning of the beam emittances, i.e. round-to-flat transformation would help to eliminate this reduction in injection efficiency. The latter has been proposed already for electrons by [1].

FLAT BEAM CREATION

Strict definition of rms-emittances is given through the transverse beam second moments matrix

$$C = \begin{bmatrix} \langle xx \rangle & \langle xx' \rangle & \langle xy \rangle & \langle xy' \rangle \\ \langle x'x \rangle & \langle x'x' \rangle & \langle x'y \rangle & \langle x'y' \rangle \\ \langle yx \rangle & \langle yx' \rangle & \langle yy \rangle & \langle yy' \rangle \\ \langle y'x \rangle & \langle y'x' \rangle & \langle y'y \rangle & \langle y'y' \rangle \end{bmatrix} \quad (1)$$

with

$$\epsilon_u := \sqrt{\langle u^2 \rangle \langle u'^2 \rangle - \langle uu' \rangle^2}, \quad (2)$$

where u stands either for x or y as the particle coordinate. The prime denotes the derivative w.r.t. the longitudinal coordinate. The eigen-emittances [2] are the two emittances to which the rms-emittances can be reduced if all inter-plane correlation moments are removed:

$$\epsilon_1 = \frac{1}{2} \sqrt{-\text{tr}[(CJ)^2] + \sqrt{\text{tr}^2[(CJ)^2] - 16\text{det}(C)}} \quad (3)$$

$$\epsilon_2 = \frac{1}{2} \sqrt{-\text{tr}[(CJ)^2] - \sqrt{\text{tr}^2[(CJ)^2] - 16\text{det}(C)}}, \quad (4)$$

where

$$J = \begin{bmatrix} 0 & 1 & 0 & 0 \\ -1 & 0 & 0 & 0 \\ 0 & 0 & 0 & 1 \\ 0 & 0 & -1 & 0 \end{bmatrix}. \quad (5)$$

The square root of the determinant of C (Equ. 1) is equal to the 4d-rms-emittance of the beam and equal to the product of the two eigen-emittances. The amount of inter-plane correlation is quantified through the coupling parameter

$$t = \frac{\epsilon_x \epsilon_y}{\epsilon_1 \epsilon_2} - 1 \geq 0. \quad (6)$$

Figure 1 depicts the EMittance Transfer EXperiment (EMTEX) beam line that performs the desired round-to-flat adoption. It comprises two doublets to provide a small double waisted beam spot in the center of a subsequent solenoid where a charge state stripping foil is inserted. It causes

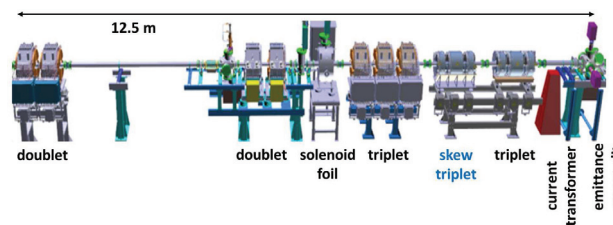


Figure 1: Beam line of EMTEx (Emittance Transfer Experiment).

Content from this work may be used under the terms of the CC BY 3.0 licence (© 2015). Any distribution of this work must maintain attribution to the author(s), title of the work, publisher, and DOI.

the solenoid entrance and exit fringe field to exert different torques to the beam, i.e. a change of its eigen-emittances as a net effect. Additionally, the solenoid causes inter-plane correlations which increase the rms-emittances. These correlations are removed by a skewed quadrupole triplet preceded by a regular triplet after the solenoid. An additional regular triplet provides for re-matching of the beam envelopes for further transport to the synchrotron. EMTEX has two very convenient features: first, the amount of residual coupling at its exit does practically not depend on the applied solenoid field B as long as the line is designed for a field B_0 satisfying $|B| \leq |B_0|$ as shown in Fig. 2. Second, the Twiss-

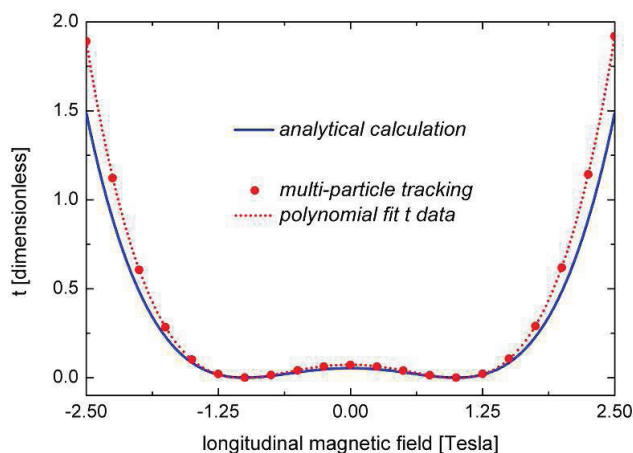


Figure 2: The coupling parameter t at the exit of EMTEX as a function of the applied solenoid field (blue line). In this example the decoupling is designed for a solenoid strength of 1.0 T.

parameters at its exit do not depend at all on the solenoid field strength. These features make EMTEX a powerful single knob emittance partitioning tool. The knob is the solenoid field strength and all other magnet settings remain constant. For detailed descriptions and for explanations on the EMTEX features we refer to [3–6].

EMTEX was commissioned using a beam of $^{14}\text{N}^{3+}$ at 11.4 MeV/u stripped to $^{14}\text{N}^{7+}$ in the solenoid. Figure 3 shows the rms-emittances measured behind EMTEX as a function of the solenoid field strength together with the values obtained from simulations [7]. The corresponding rms-ellipses are plotted in Fig. 4. It shows that the shapes and orientations of the ellipses remain constant. During the measurements just the solenoid field has been changed, all other settings remained constant. Accordingly, simple single-knob emittance partitioning under preservation of the envelope parameters α and β was demonstrated. This feature is very convenient for later application of this beam as injection into a ring. By inversion of the solenoid field or the gradients of the skew gradients the emittance ratio can be inverted as being indicated for horizontal MTI. The experiments are described in detail in [8].

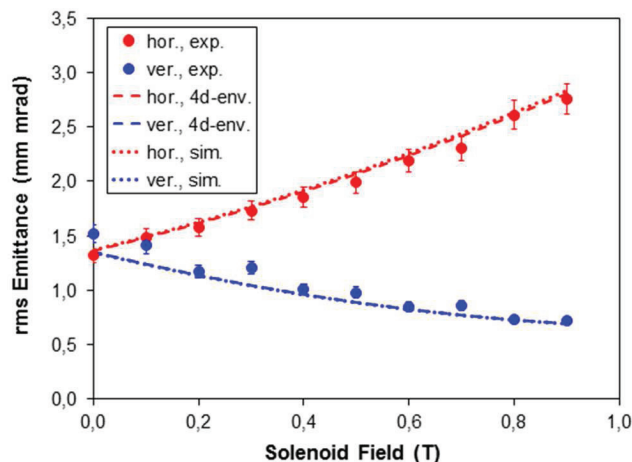


Figure 3: Vertical (blue) and horizontal (red) rms emittances at the exit of the EMTEX beam line as functions of the solenoid field strength. All other settings were kept constant. Shown are results from measurements (dots), from application of the 4d-envelope model for coupled lattices (dashed) [7], and from tracking simulations (dotted).

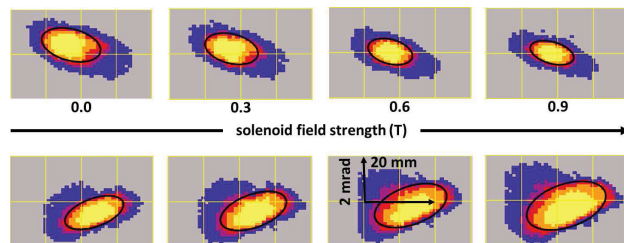


Figure 4: Vertical (upper) and horizontal (lower) phase space distributions measured at the exit of the EMTEX beam line as functions of the solenoid field strength. All other settings were kept constant. Black ellipses indicate the $4 \times$ rms ellipses.

MULTI-TURN INJECTION

In SIS18, the injected beamlets are stacked in the horizontal phase space until the machine acceptance is reached. To fulfill Liouville's theorem, four bumper magnets create a time variable closed orbit bump such that the electrostatic injection septum deflects the next incoming beamlet into free horizontal phase space and close to the formerly injected beamlets. The performance of the MTI is determined by the number of accumulated beamlets and the associated loss. If η characterizes the ratio between the lost and injected particles it follows for the multiplication factor

$$m = n(1 - \eta). \quad (7)$$

For a loss free injection η is zero and the effectively accumulated beamlets m are equal to the number of injected turns n . The number of injected turns is controlled through the injection time and is given by the ratio of injection to revolution time.

To achieve high beam intensities the injected beamlets should be packed as compact as possible. In normalized

phase space coordinates the injected beamlets as well as the beam pipe are approximately circular, therefore the MTI packing problem is similar to the packing of ropes and cables. Assuming that m beamlets with radius a are packed into a given machine acceptance A (or container) with radius R (also named hexagonal packing) and imagine hexagons which circumscribe those beamlets. Then the number of beamlets is defined as [9]

$$m = \frac{2\sqrt{3} R^2}{\pi d a^2} = \frac{2\sqrt{3} A_x}{\pi d \epsilon_x}. \quad (8)$$

The hexagonal packing of circles onto an annular ring leads to a shell structure and the dilution d will be larger than one [10].

The above equation demonstrates clearly for a given horizontal machine acceptance a smaller horizontal emittance of the incoming beam results in a larger number of accumulated beamlets. As demonstrated in [11] reduction of the horizontal emittance by horizontal collimation can lead to a better MTI performance. In addition, horizontal collimation of the beam already along the transfer line will allow controlled anticipation of beam loss, i.e. mitigate unavoidable loss in the synchrotron which is harmful to the vacuum.

The benefit to the MTI performance of the reduced horizontal emittance to the emittance transfer in the linac has been investigated in a selected beam experiment. As shown in [12] reduced horizontal emittance directly translates into increased MTI efficiency (Fig. 5). Shown are cases for different amounts of transverse beam flatness which is defined exclusively by the solenoid field strength. The smaller injected emittance leads directly to a reduction of the injection loss, since the injection time i.e. the number of injected turns has not been extended. Other parameters like the closed orbit bump reduction as been adopted on the different injection emittance.

OUTLOOK

For a further quantification of the achievable gain factor of the MTI performance by EMTEX the limits of this technique should be further investigated. This could be done by increasing the macro pulse length, i.e. the injection time, above 150 μs regularly used and by increasing the beam intensity from the source.

EMTEX was demonstrated for beams that are stripped into one single charge state and that are not prone to space charge effects. Simulations showed that the technique can also be applied to intense beams of heavy ions being stripped to a broad spectrum of charge states. These simulations are under refinement aiming at a dedicated beam line that can provide adjustable round-to-flat adoption for all ion species provided at GSI.

In order to further improve the MTI performance a genetic algorithm based optimization is used to simultaneously minimize the loss, maximize the multiplication factor (e.g. stored currents in the synchrotron), and to minimize the required linac brilliance [13]. Besides the emittance of the

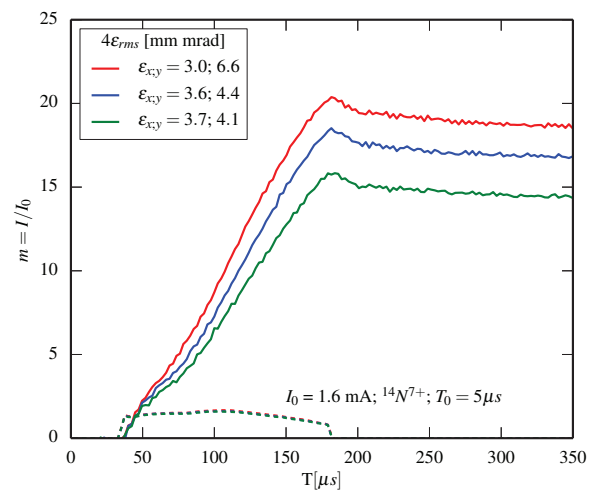


Figure 5: Measured beam current in the transfer line to the synchrotron (dashed) and in the synchrotron itself (solid) as a function of time during the horizontal multi-turn injection. Shown are cases for different amounts of transverse beam flatness which is defined exclusively by the solenoid field strength.

injected beam the genetic algorithm alters also other MTI-dependent parameters like the distance of the beam center to the septum, the slope of the injected beam, the closed orbit bump reduction, the number of the injection periods, and the number of betatron oscillations per turn Q .

REFERENCES

- [1] R. Brinkman et al., PRSTAB 4, 053501 (2001).
- [2] A.J. Dragt, PR 45, 4 (1992).
- [3] L. Groening, PRSTAB 14, 064201 (2011)
- [4] C. Xiao et al. PRSTAB 16, 044201 (2013)
- [5] C. Xiao et al. Proc. HB2012 Workshop (2012).
- [6] L. Groening et al. arXiv:1403.6962 (2014).
- [7] Moses Chung et al., Phys. Plasma 22, 013109 (2015)
- [8] L. Groening et al., PRL 113, 264802 (2014).
- [9] S. Kravitz, Mathematics magazine 40 (2) (1967).
- [10] Chao, A, Handbook of accelerator physics and engineering, ISBN: 978-981-4415-84-2 World Scientific Publishing, (1999).
- [11] Y. Hayek, PhD thesis Uni Frankfurt (2013).
- [12] S. Appel, GSI Report 2013-03 (2013).
- [13] S. Appel et al., in Proc. of IPAC 2015, (2015).